Stability Ordering of Cycle Expansions

C. P. Dettmann and G. P. Morriss
School of Physics, University of New South Wales, Sydney 2052, Australia
(Received 3 December 1996)

We propose that cycle expansions be ordered with respect to stability rather than orbit length for many chaotic systems, particularly those exhibiting crises. This is illustrated with the strong-field Lorentz gas, where we obtain significant improvements over traditional approaches. [S0031-9007(97)03297-3]

PACS numbers: 05.45.+b, 05.70.Ln

Classical chaotic dynamical systems are inherently unpredictable, so that even if the initial conditions are known with high accuracy, predictions of the state of the system may be made to only a short time of order λ_1^{-1} in the future, where λ_1 is the largest Lyapunov exponent. Despite this unpredictability, much can be said about the average behavior of the system in many cases using only a small number of unstable periodic orbits or "cycles." This can be achieved by using cycle expansions [1,2] of Ruelle's dynamical zeta function [3].

Cycle expansions have proved very useful in both classical and quantum chaos, giving accurate estimates of the escape rate of open billiard systems [4] and the energy levels of helium [5] using a surprisingly small number of classical cycles. The main idea of this approach is that a long generic trajectory may be approximated by various periodic orbits at different times, and that longer periodic orbits may often be "shadowed" by shorter "fundamental" cycles, closely following the shorter cycles along different sections of its length. Thus averages are calculated using fundamental cycles, with small corrections due to longer cycles. Periodic orbits which are exact repetitions of smaller cycles are explicitly summed, so that all expressions are written in terms of the remaining "prime" cycles. The expansions work best when the symbolic dynamics is well understood, and long periodic orbits are well shadowed by shorter ones. In this paper we investigate a system in which neither of these conditions holds, the strong-field Lorentz gas. In spite of these difficulties, reasonable results may be obtained by ordering the expansion in terms of stability rather than the length of periodic orbits. This approach should be valid wherever cycle expansions can be applied, including flows for which a natural topological "length" is difficult to define.

The origin of cycle expansions is a well developed theory of trace formulas and dynamical zeta functions [3,6]. Here we will need only the expression for the classical time average of some quantity A in a closed system [2],

$$\langle A\rangle_t = \frac{\sum(-1)^k(A_1\tau_1 + \cdots + A_k\tau_k)/(\Lambda_1\cdots\Lambda_k)}{\sum(-1)^k(\tau_1 + \cdots + \tau_k)/(\Lambda_1\cdots\Lambda_k)}. \quad (1)$$

The sum is over all distinct nonrepeating combinations of prime cycles, τ is the period of a cycle, and Λ is magnitude of the expanding eigenvalue of the stability matrix, equal to $\exp(\tau\sum\lambda_+)$, where $\sum\lambda_+$ is the sum of the positive Lyapunov exponents. Note that for notational simplicity we have written Λ where other authors have $|\Lambda|$. A_i is the average of some quantity over a particular orbit, and could be Lyapunov exponent, current, or the number of collisions per unit time. An important check of the convergence of the expansion is given by

$$\zeta(0,0)^{-1} = 1 + \sum(-1)^k/(\Lambda_1\cdots\Lambda_k), \quad (2)$$

which should be equal to zero for a closed system.

The sums are usually truncated up to a particular order in the symbolic dynamics: for the Lorentz gas, the number of collisions N. At each order the terms are grouped into fundamental orbits that have a symbolic dynamics not separable into smaller cycles, and "curvature corrections" consisting of a composite orbit, with symbolic dynamics ab together with its components a and b. Often the composite orbit has similar averages to its components; then the combined term $-A_{ab}\tau_{ab}\Lambda_{ab}^{-1} + (A_a\tau_a + A_b\tau_b)\Lambda_a^{-1}\Lambda_b^{-1}$ is small. If there are only a few fundamental orbits and this cancellation occurs most of the time the cycle expansion converges rapidly as a function of N. However, this is often not the case, as we see for the Lorentz gas (Table I below).

Occasionally, cycle expansions are truncated using different criteria. The most notable is that of Dahlqvist and

TABLE I. The shortest cycles at a field $\epsilon = 2.4$. Note the lack of shadowing, in that $\Lambda_{244426} \gg \Lambda_{2444}\Lambda_{26}$. Also, Λ is not strongly correlated with N, so that truncating a cycle expansion at fixed N tends to omit significant orbits with small Λ.

N	Symbolic dynamics	Λ	τ
2	26	13.92	1.459
3	264	2.557	2.706
4	2444	5.337	2.786
5	26264	60.50	4.133
5	24426	175.6	3.061
6	244426	736.6	4.147
7	2442644	1.536	5.763
7	2444264	37.16	5.471
7	2626264	907.9	5.594

 © 1997 The American Physical Society

Russberg [7], who use the magnitude of the terms in an expansion. This has the advantage that it is independent of the symbolic dynamics, but applied to Eq. (1) it has a number of disadvantages. It depends on A, so a different set of orbits is required for each observable; it orders the numerator and denominator of Eq. (1) differently, and is not directly related to a cycle data set, which is more likely truncated according to orbit stability Λ.

We suggest that the orbit stability Λ may often be the most convenient parameter with which to truncate the cycle expansions. There are a number of reasons for this. The cycles which make the greatest contribution to the expansions have small Λ, which are not necessarily those of small N. The cycles of smallest Λ are also found most readily in numerical searches. Alternative methods for enumerating periodic orbits by exhaustive enumeration of symbol sequences (as in the zero field Lorentz gas [8]) fail whenever the symbolic dynamics is not understood completely and cycles exist which are not contained in the chaotic set. This is the case on one side of a chaotic crisis. See Chap. 8 of Ref. [9], where a number of examples are discussed, including the windows of the logistic map, and the Lorenz attractor. Another reason for truncating in Λ rather than N is that there may be significant cycles (small Λ) at comparatively large N. Continuing the expansion to include all cycles at large N may be prohibitive due to the large number of cycles, or that some of the cycles may have very large Λ and hence pose numerical problems. These issues are illustrated by our study of the strong-field Lorentz gas.

We now make the above prescription more precise. To retain the exponential convergence of traditional cycle expansions, it is clear that we must still make use of the close cancellation of curvature correction terms. This comes naturally if we include all terms for which the product of Λ's is less than a predetermined cutoff $\Lambda_{\max}$. Then, if the product of Λ's match, the canceling terms will be either included or excluded together. If the shadowing is poor, cancellation would not occur, whichever terms are included. In any case, it is clear that the expansions will not work well if cycles are missing, whether the expansion is ordered with respect to N or Λ. Our prescription is thus:

Alternative truncation of cycle expansions: only those cycles and combination of cycles which have the product of Λ's less than a cutoff $\Lambda_{\max}$ should be included in the cycle expansion. $\Lambda_{\max}$ is the largest value such that almost all the cycles are known.

For the remainder of this paper we show how this works for the strong-field Lorentz gas, obtaining significantly improved convergence.

The two dimensional nonequilibrium Lorentz gas is a classical model of current flow in a conductor, and shares many of the properties of larger steady state nonequilibrium systems, including a simple relationship between the steady state current, and the sum of the Lyapunov exponents $\mathbf{J} \cdot \mathbf{E} = \sum \lambda$ [10]. Here, $\mathbf{E}$ is the imposed electric field. A single particle of charge e is scattered by a triangular lattice of circular disks of radius 1 and nearest neighbor spacing 0.236. Between collisions it moves according to the equations

$$\dot{\mathbf{x}} = \mathbf{v}, \qquad \dot{\mathbf{v}} = e\mathbf{E}/m - \alpha\mathbf{v}, \tag{3}$$

where $\alpha = e\mathbf{v} \cdot \mathbf{E}/mv^2$ is a Gaussian thermostatting coefficient [11] which keeps the kinetic energy constant, permitting the system to reach a steady current $\mathbf{J} = \langle e\mathbf{v} \rangle_t$. The symbolic dynamics is determined by the sequence of disks with which the particle collides; see Fig. 1.

For small fields $\epsilon = |e\mathbf{E}/m| \ll 1$ the dynamics is known to be ergodic and leads to a steady current [12]. There have been several previous investigations [8,13] of the Lorentz gas at zero field (equilibrium) and small fields using both cycle expansions (above) and direct calculation of measures based on periodic orbits. They used 10^3–10^5 cycles to evaluate the largest Lyapunov exponent, the diffusion coefficient (for zero field), and the current (for nonzero field). In each case the expansions were evaluated to a particular orbit length N, from 7 to 10. Most of the results have uncertainties of 5%–10%, the main exception being the evaluation of the Lyapunov exponent in Ref. [8], which has an uncertainty of about 0.2%. This last calculation was performed in the fundamental domain, making full use of the symmetry of the lattice. The convergence for the Lorentz gas calculations is not as impressive as that in Refs. [4,5] because the grammar of the symbolic dynamics, that is, the rules determining which symbol sequences occur, is not well understood. Thus the amount to which longer orbits are shadowed by shorter ones is limited.

At a field of $\epsilon = 2.2$ the ergodic attracting measure is abruptly replaced by an attractor with fractal support characterized by a very restricted symbolic dynamics [14]. In particular (see Fig. 1), the only symbols are $\{2, 4, 6, 8, \underline{10}\}$, the allowed pairs of symbols are $\{26, 28, 48, 4\underline{10}, 62, 64, 68, 6\underline{10}, 82, 84, \underline{10}4, \underline{10}6\}$, and the triples $\{262, 264, \underline{10}68, \underline{10}6\underline{10}\}$ are prohibited. These rules

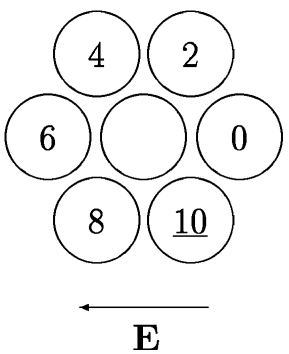

FIG. 1. The symbolic dynamics for the Lorentz gas at high field, for which only nearest neighbor collisions occur. We reduce the symbol set still further by noting that $\underline{10}$ is equivalent to 2 by symmetry, and similarly 8 is equivalent to 4.

determine that the particle moves in one direction along a channel formed by the disks, as described in Ref. [14]. Making use of the fact that the system is invariant under a reflection in the x axis, we note that the symbols 2 and $\underline{10}$ are equivalent, and likewise 4 and 8. Thus the above permitted sequences become $\{24, 26, 42, 44, 62, 64\}$, with no restrictions on the triples. It is easy to check that each symbol sequence of the restricted set corresponds to exactly two equivalent sequences with the original symbols. Note that there are many other prohibited sequences of three or more symbols, depending on the field, so this system suffers from pruning in a similar fashion to the small field case. The range of fields we consider is 2.2 to 2.4, above which stable orbits appear, rendering the attractor nonhyperbolic.

The symbolic dynamics of this system is so restricted that at $\epsilon = 2.4$ there are only nine orbits with seven or fewer collisions; see Table I. There are a couple of points to note from this table. First, there is very little shadowing of orbits. Five of the cycles are fundamental in that they cannot be constructed from smaller cycles. In addition, the cycles that can be constructed from smaller cycles do not have eigenvalues Λ which are close to the product of the constituent Λ's, so curvature corrections obtained with these orbits are not particularly small. Secondly, the most significant orbits (with small Λ) do not occur at small N. There are two $N = 10$ orbits more significant than the $N = 2$ orbit, and 20 orbits with $\Lambda < 100$, including one with $N = 34$. Most of the longer orbits are partly canceled in curvature corrections, but it is clear from the numerical results (below) that they are necessary to obtain optimal convergence.

It is clear that obtaining all periodic orbits with fewer than, say, 30 collisions is quite unfeasible, since $N = 7$ is already approaching the limit. In any case, this is not in line with the basic philosophy of describing the dynamics with as few cycles as possible. Thus we proceed to truncate the expansions using Λ rather than N.

We numerically generated 10^5 collisions for each of the field values from 2.2 to 2.4 in steps of 0.001, searching for periodic orbits of up to $N = 40$. This generates about 170 cycles for each field value, substantially fewer than Refs. [8,13], which considered a much smaller number of field and disk spacing values. Seven of the orbits in Table I were found, those with the smallest Λ. To get a more precise estimate of the Λ value at which cycles are first being missed, we plot the logarithm of the total number of cycles found as a function of $\ln \Lambda$ in Fig. 2. The graph turns sharply down at about $\Lambda = 600$, indicating that the optimum $\Lambda_{\max}$ should be around this value.

We computed $\zeta(0,0)^{-1}$ using Eq. (2) at each field value summing terms up to different values of N and $\Lambda_{\max}$, and also evaluated the Lyapunov exponents λ_1, λ_2, and the current J using Eq. (1) under the same conditions. The rms averaged $\zeta(0,0)^{-1}$ values are shown in Fig. 3. The cycle expansion values for λ_1, λ_2, and J were then compared with direct simulation results at each field value, to give the rms differences exhibited in Table II.

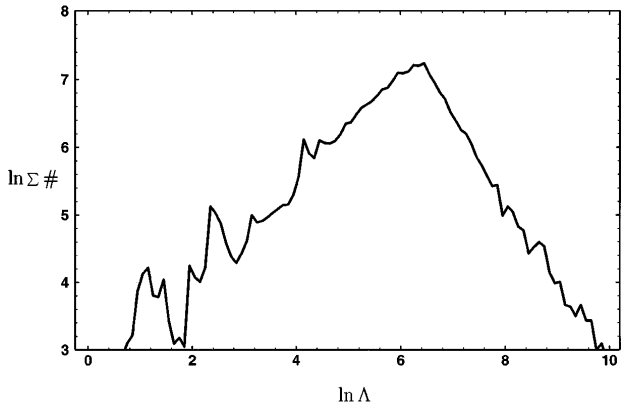

FIG. 2. The distribution of cycles found using our numerical routine, using bins of equal size in terms of $\ln \Lambda$. The maximum occurs at about $\Lambda = 600$, suggesting this as the optimal value of $\Lambda_{\max}$.

From Fig. 3 we note that for each value of the cutoff there is an initial regime in which convergence is exponential with N, as usual for cycle expansions in hyperbolic systems [2]. At $\Lambda_{\max} = 600$ this holds to about $N = 24$, while at $\Lambda_{\max} = \infty$ (no cutoff) convergence is exponential only to $N = 15$. Subsequently, the behavior is determined by the limitations of the data set. If almost all of the cycles are present (as for $\Lambda_{\max} < 600$), the normalization improves slightly, and then remains constant, otherwise it gets worse. A cutoff which is too high ($\Lambda_{\max} = 10^4$) can be more harmful than no cutoff, presumably because the unbalanced corrections at $600 < \Lambda < 10^4$ are partly canceled by the more numerous terms with opposite signs at larger Λ.

The results for the Lyapunov exponents and the current (Table II and Fig. 4) are more or less what would be

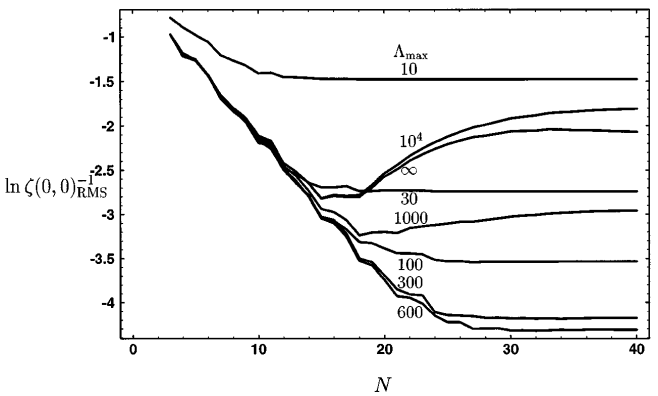

FIG. 3. Superior normalization of cycle expansions with stability cutoff, using Eq. (2). All expansions with $\Lambda_{\max} > 10$ converge exponentially to $N = 15$, after which the expansion with no cutoff ($\Lambda_{\max} = \infty$) diverges slightly, while the optimal cutoff ($\Lambda_{\max} = 600$) continues to improve up to $N = 30$.

TABLE II. Cycle expansion results, showing the average number of periodic orbits used, $\#_{\text{av}}$, and the rms differences of the other quantities from the direct simulation results. All contributions up to $N = 40$ are included. The best convergence is obtained with $\Lambda_{\max} = 600$, a factor of 3 better than no cutoff ($\Lambda_{\max} = \infty$).

$\Lambda_{\max}$	$\#_{\text{av}}$	$\zeta(0,0)^{-1}_{\text{rms}}$	$\Delta\lambda_{1\text{-rms}}$	$\Delta\lambda_{2\text{-rms}}$	ΔJ_{rms}
10	3.7	0.2283	0.0559	0.0865	0.0249
30	10.2	0.0647	0.0648	0.0774	0.0136
100	26.8	0.0292	0.0226	0.0312	0.0061
300	62.9	0.0153	0.0095	0.0125	0.0029
600	104.0	0.0134	0.0074	0.0102	0.0025
1000	131.1	0.0519	0.0162	0.0205	0.0039
10000	157.6	0.1640	0.1814	0.1525	0.0256
∞	169.2	0.1264	0.0190	0.0331	0.0083

predicted from the normalization, except that the $\Lambda_{\max} = \infty$ results are unexpectedly good, and comparable to $\Lambda_{\max} = 100$. Given that $J \approx 0.7$, the relative error in the cycle expansion expression for J at $\Lambda_{\max} = 600$ is about 0.3%, comparable to the best results in Ref. [8], which required an order of magnitude more cycles.

Finally, we use the results for $\zeta(0,0)^{-1}$ to estimate the rate of convergence of the expansion when almost all the cycles are known, that is $\Lambda_{\max} < 600$. Note that because a hyperbolic system has $\Lambda \sim e^N$, exponential convergence in N is equivalent to exponential convergence in $\ln \Lambda_{\max}$, that is a power law in $\Lambda_{\max}$. This is shown in Fig. 5, where we find $\zeta(0,0)^{-1}_{\text{rms}} \sim \Lambda_{\max}^{-0.69}$, or $\zeta(0,0)^{-1}_{\text{rms}} \sim 2^{-\ln \Lambda_{\max}}$. The rate of convergence is thus comparable with that of cycle expansions performed up to a given N. The choice of which approach to take depends on whether it is more convenient to enumerate all orbits to a fixed N or a fixed Λ, and the distribution of periodic orbits for the given system.

It would be interesting to compare this method with the traditional approach for other classical systems, and also quantum systems, where formulas such as Eq. (1) are replaced by more involved expressions, but still written in terms of classical periodic orbits. It could also be applied to flows for which no natural Poincaré section is known. This work was supported by the Australian Research Council.

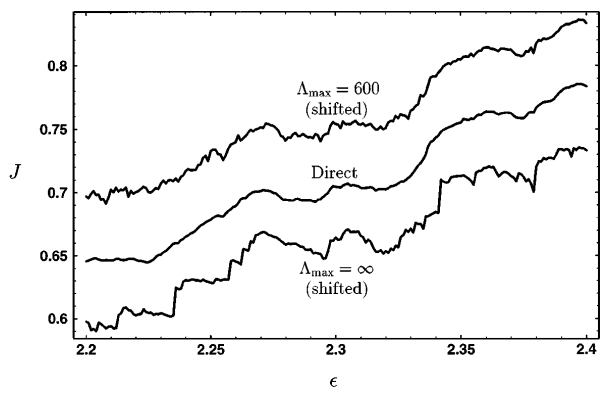

FIG. 4. The current at high field (center). Note the high degree of structure, which is reproduced in the cycle expansions with $\Lambda_{\max} = 600$ (top) and to a lesser degree $\Lambda_{\max} = \infty$ (bottom). The cycle expansion results are shifted by 0.05 for clarity.

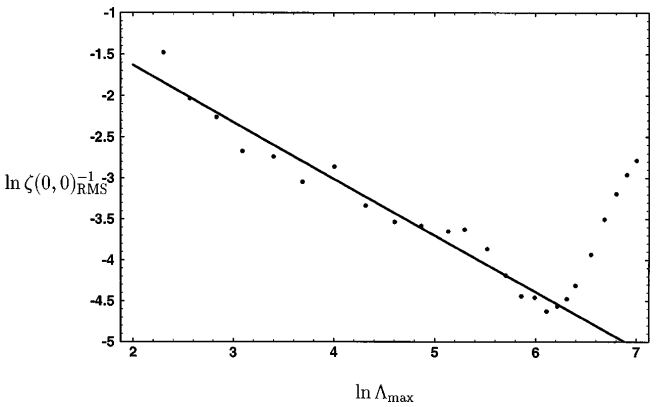

FIG. 5. The normalization at $N = 40$ as a function of $\ln \Lambda_{\max}$ showing exponential convergence up to $\ln \Lambda_{\max} \approx 6.3$. The solid line has a gradient of -0.69.

[1] P. Cvitanović, Phys. Rev. Lett. **61**, 2729 (1988).
[2] R. Artuso, E. Aurell, and P. Cvitanović, Nonlinearity **3**, 325 (1990); **3**, 361 (1990).
[3] D. Ruelle, *Statistical Mechanics, Thermodynamic Formalism* (Addison-Wesley, Reading, Massachusetts, 1978); J. Stat. Phys. **44**, 281 (1986).
[4] P. Cvitanović and B. Eckhardt, Phys. Rev. Lett. **63**, 823 (1989); P. Gaspard and D. Alonso Ramirez, Phys. Rev. A **45**, 8383 (1992); G. Vattay, A. Wirzba, and P. E. Rosenquist, Phys. Rev. Lett. **73**, 2304 (1994).
[5] D. Wintgen, K. Richter, and G. Tanner, Chaos **2**, 19 (1992).
[6] M. C. Gutzwiller, *Chaos in Classical and Quantum Mechanics* (Springer-Verlag, New York, 1990).
[7] P. Dahlqvist and G. Russberg, J. Phys. A **24**, 4763 (1991); P. Dahlqvist, J. Phys. A **27**, 763 (1994).
[8] P. Cvitanović, P. Gaspard, and T. Schreiber, Chaos **2**, 85 (1992).
[9] E. Ott, *Chaos in Dynamical Systems* (Cambridge University, Cambridge, 1993).
[10] B. Moran and W. G. Hoover, J. Stat. Phys. **48**, 709 (1987); J. Lloyd, M. Niemeyer, L. Rondoni, and G. P. Morriss, Chaos **5**, 536 (1995).
[11] D. J. Evans and G. P. Morriss, *Statistical Mechanics of Nonequilibrium Liquids* (Academic, London, 1990).
[12] N. I. Chernov, G. L. Eyink, J. L. Lebowitz, and Ya. G. Sinai, Commun. Math. Phys. **154**, 569 (1993).
[13] W. N. Vance, Phys. Rev. Lett. **69**, 1356 (1992); G. P. Morriss and L. Rondoni, J. Stat. Phys. **75**, 553 (1994).
[14] C. P. Dettmann and G. P. Morriss, Phys. Rev. E **54**, 4782 (1996).